Boundary-Layer Meteorology manuscript No.
(will be inserted by the editor)

A note on spatial averaging and shear stresses within urban canopies

Zheng-Tong Xie · Vladimir Fuka

Received: date / Accepted: date

Abstract One-dimensional urban models embedded in mesoscale models may place a few grid points within the urban canopy. This requires an accurate parametrization for shear stresses (i.e. vertical momentum fluxes) including dispersive stress and momentum sinks at these points. We used a case study with a packing density 33% and checked rigorously the vertical variation of spatially averaged total shear stress, which can be used in a one-dimensional column urban model. We found that the intrinsic spatial average, in which the volume or area of the solids parts were not included in the average process, yielded greater time-spatial average of total stress within the canopy and a more evident abrupt change at the top of the buildings than the comprehensive spatial average, in which the volume or area of the solids parts were included in the average.

Keywords Comprehensive spatial average · Effective total shear stress · Intrinsic spatial average · One-dimensional column urban model · Vertical momentum flux

1 Introduction

The horizontal resolution of operational mesoscale models is now around 1km for a few hundreds of kilometres computational domain including urban areas. It is urgently required to have a more accurate parametrization of air flows within the urban canopy 'representing aggregate effects of heterogeneous urban elements as subgrid processes (Fernando, 2010)', so as to estimate vertical profiles of effective total shear stress, turbulent shear stress, dispersive shear stress and vertical distributions of drag coefficient, heat source and scalar sources at a few levels per average building height

Zheng-Tong Xie · Vladimir Fuka
Facultu of Engineering and Environment
University of Southampton
Tel: +44(0)23 8059 4493
Fax: +44(0)23 8059 3058
E-mail: z.xie@soton.ac.uk

in one-dimensional column urban models (e.g. Martilli, 2002; Kondo et al., 2005; Santiago and Martilli, 2007; Masson and Seity, 2009; Martilli and Santiago, 2010; Husain et al., 2013; Gutierrez et al., 2015; Sharma et al., 2017). It is even more important for parametrization over an urban area with densely placed high-rise buildings. Note the effective total shear stress is the sum of all shear stress components including the converted form (pressure) drag and viscous drag due to the buildings, denoted by 'total shear stress' or 'total stress' thereafter.

The spatial averaging procedure needs to be designed to estimate these shear stresses (i.e. vertical momentum fluxes) including dispersive stress and momentum sinks (i.e. drag) in one-dimensional column urban models. We thereafter consider the term 'vertical momentum flux' with a unit m^2s^{-2} is equivalent to the term 'shear stress', while the term 'total vertical momentum flux of the computational domain' with a unit m^4s^{-2} is equivalent to the term 'total shear force'. The term 'dispersive flux' or 'dispersive stress' was introduced about half a century ago (e.g. Gray, 1975; Wilson and Shaw, 2007). Wilson and Shaw (2007) used dispersive stress to develop a one-dimensional numerical model for air flows within vegetative canopies. The dispersive stress is the vertical momentum flux extracted from air flow at a certain height to the level below or above, which is due to spatial variations of the local time-averaged velocities calculated using spatial averaging over a horizontal plane. These are analogues of the Reynolds stresses, while the latter are cross-correlations of turbulent fluctuations usually calculated using time averaging at one point.

There is a debate on whether the averaging volume excludes or includes the solid parts. Eq. 1 shows the former,

$$\langle \phi \rangle_I (z) = \frac{1}{S_f} \int_{S_f} \phi(x,y,z) \mathrm{d}x\mathrm{d}y, \tag{1}$$

where ϕ is a flow quantity, such as velocity, stress, heat flux and scalar flux; $\langle\rangle$ denotes spatial averaging; S_f is the fluid area. $\langle \phi \rangle_I$ is known as the intrinsic spatial average (ISA) (e.g. Slattery, 1999), which is widely used in the literature, such as, Gray (1975), Wilson and Shaw (2007), Raupach and Shaw (1982), Raupach et al. (1986), Finnigan (2000), Coceal et al. (2006), Nikora et al. (2007) and Xie et al. (2008).

Eq. 2 shows the averaging volume including the solid parts,

$$\langle \phi \rangle_c (z) = \frac{1}{S_c} \int_{S_f} \phi(x,y,z) \mathrm{d}x\mathrm{d}y, \tag{2}$$

where S_c is the total area including that occupied by solid; $\langle \phi \rangle_c$ is defined here as the comprehensive spatial average (CSA).

So far only a very few papers report that the CSA is used. Yuan and Piomelli (2014) choose the CSA to analyze the momentum flux budgets in turbulence within and above a group of randomly rotated ellipsoids. Their numerical data were obtained using direct numerical simulation (DNS) with an immersed boundary method (IBM) to represent the ellipsoids, and the spatially averaged vertical profiles of components of vertical momentum flux show an excellent consistency below and immediately above the roughness crest.

Recently we used large-eddy simulations (LES) to calculate flows over a group of aligned cuboids with a packing density 33% (Castro et al., 2016). When using the ISA, we noticed in this case study that, (1) the time- and spatially-averaged vertical profile of total shear stress shows an abrupt change at the canopy height; (2) the total shear stress immediately below the canopy height is much greater than that immediately above the canopy; (3) the magnitude of the total shear stress within the canopy calculated from the ISA approach is much greater than that from the CSA approach. This may cause serious problems for parametrization of momentum flux, drag coefficient, heat source and scalar source for one-dimensional column urban model in mesoscale models if no attention is paid. This short paper focuses on this issue and attempts to give a suggestion.

2 Case study

We focus on a case study (see Fig. 1b) that similates flows over a group of aligned cuboids with a packing density 33% (Castro et al., 2016). Large-eddy simulation was used with governing equations,

$$\frac{\partial u_i}{\partial t}+\frac{\partial u_i u_j}{\partial x_j}=-\frac{\partial}{\partial x_i}\left(\frac{p}{\rho}\right)+\frac{\partial}{\partial x_j}\left(\nu\frac{\partial u_i}{\partial x_j}\right)+\frac{\partial}{\partial x_j}\left(-\widehat{u_i'' u_j''}\right)-\delta_{i1}\frac{\partial}{\partial x_i}\left(\frac{P}{\rho}\right). \quad (3)$$

The resolved velocity and pressure are respectively given by u_i and p with $u(u_1)$, $v(u_2)$ and $w(u_3)$ the streamwise, lateral and vertical velocity components respectively. u_i'' is the subgrid-scale (SGS) velocity. The last term $-\delta_{i1}\frac{\partial}{\partial x_i}\left(\frac{P}{\rho}\right)$ is the specified driving body force, ρ and ν are the density and kinematic viscosity of the fluid, $\widehat{\ }$ denotes filtering in subgrid, $-\widehat{u_i'' u_j''}$ is the SGS stress and is handled using the mixing time scale model (Inagaki et al., 2005).

The domain length and width are significantly less than those of the wind tunnel model (Fig. 1a) placed in a simulated boundary layer. The domain height is $12h$, which is slightly less than the boundary layer height $14h$ in the wind tunnel. The LES data are validated using the wind tunnel measurements in Castro et al. (2016).

On the top of the domain, stress-free boundary conditions are specified, i.e.,

$$\frac{\partial u}{\partial z}=\frac{\partial v}{\partial z}=0; \quad w=0. \quad (4)$$

Periodic boundary conditions were specified in the streamwise and lateral directions. A constant pressure gradient $-\delta_{i1}\frac{\partial}{\partial x_i}\left(\frac{P}{\rho}\right)$ is used to drive the flows, which can also be seen as a body force in the fluid. Using periodic boundary conditions in the horizontal directions and knowing the exact driving force are the key to assessing the budget of the vertical momentum flux, and this is the focus of this note. The cuboid surfaces and the floor are defined as non-slip walls, and are expected to contribute to 100% of the total drag, which is equal to the integration of the driving body force.

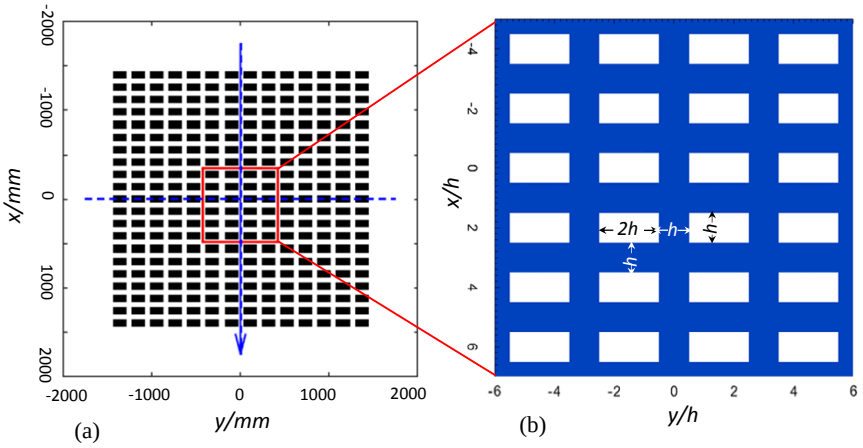

Fig. 1 Arrays of aligned cuboids with dimensions $2h$ (length) $\times$ h (width) $\times$ h (height). All spacings between the cuboids are h, with $h = 70$ mm. The Reynolds number based on cuboid height and the velocity at that height in the upstream boundary layer in the wind tunnel was about 7,400. (a) wind-tunnel model. (b) numerical model in a computational domain $12h$ (L_x) $\times$ $12h$ (L_y) $\times$ $12h$ (L_z) with periodic boundary conditions in horizontal directions.

3 Spatially averaged stresses

Using the ISA over the whole (x-y) plane (Fig. 1), a resolved instantaneous flow quantity ϕ in LES can be further decomposed into space-time average $\langle\overline{\phi}\rangle$, spatial variation of the time average $\tilde{\phi}$, and resolved turbulence fluctuation ϕ' which is the deviation of the resolved instantaneous quantity ϕ from the time average $\overline{\phi}$,

$$\phi = \langle\overline{\phi}\rangle + \tilde{\phi} + \phi', \tag{5a}$$

$$\text{and} \quad \overline{\phi} = \langle\overline{\phi}\rangle + \tilde{\phi}. \tag{5b}$$

Applying the ISA to the time-averaged u-momentum equation of Eq. 3 for (x-y) planes of the computation domain in Fig. 1b, we obtain,

$$-\left\langle\frac{\partial P}{\rho\partial x_1}\right\rangle-\left\langle\frac{\partial\overline{p}}{\rho\partial x_1}\right\rangle+\left\langle\frac{\partial}{\partial x_j}\left(\nu\frac{\partial\overline{u_i}}{\partial x_j}\right)\right\rangle-\left\langle\frac{\partial\overline{u_1}\,\overline{u_3}}{\partial x_3}\right\rangle-\left\langle\frac{\partial(\overline{u_1'u_3'}+\widehat{\overline{u_1''u_3''}})}{\partial x_3}\right\rangle=0. \tag{6}$$

Following Yuan and Piomelli (2014), and considering Eq. 5 and using the CSA to substitute the ISA process, Eq. 6 can be written as,

$$-\frac{\partial \langle P \rangle_c}{\rho \partial x_1} - \left\langle \frac{\partial \tilde{p}}{\rho \partial x_1} \right\rangle_c + \nu \frac{\partial^2 \langle \overline{u_1} \rangle_c}{\partial x_3^2}$$
$$+\nu \left\langle \frac{\partial^2 \tilde{u}_1}{\partial x_i^2} \right\rangle_c - \frac{\partial \langle \tilde{u}_1 \tilde{u}_3 \rangle_c}{\partial x_3} - \frac{\partial \left\langle \overline{u_1' u_3'} + \widehat{\overline{u_1'' u_3''}} \right\rangle_c}{\partial x_3} = 0, \tag{7}$$

where the first term is the constant pressure gradient, the second and fourth terms are respectively the form (pressure) and viscous drag forces imposed by the solid parts (e.g. Wilson and Shaw, 2007; Raupach and Shaw, 1982; Yuan and Piomelli, 2014), the third term is the viscous shear due to vertical gradient of the time- and spatially-averaged velocity, the fifth term is the dispersive shear stress, and the last term is the turbulence shear stress.

It is not trivial to calculate the second and fourth terms in Eq. 7. For the case shown in Fig. 1, we discretised the block height evenly into 16 horizontal slices with a thickness $h/16$. The pressure and viscous drag forces on the cuboid surfaces within each slice were converted into an increment of shear stress over that slice. The integration of these increments from the cuboid top to a certain height is the integrated drag contribution (i.e. 'integrated drag stress' in Fig. 2) to the effective total time- and spatially-averaged shear stress at that height, denoted by 'total shear stress' or 'total stress'.

We plot vertical profiles of the stresses rather than vertical gradients as the terms in Eq. 7, because the former shows a more evident shape, such as the total shear stress in a linear profile above the canopy given that a constant driving body force in imposed. Researchers (e.g. Martilli, 2002; Kondo et al., 2005; Husain et al., 2013) usually use a body force to take into account the effects of buildings applied in various layers in the one-dimensional column models. These body forces can be calculated from an estimated vertical profile of the integrated drag stress.

Fig. 2 shows vertical profiles of time- and spatially-averaged total shear stress, Reynolds shear stress, dispersive stress, integrated drag stress, viscous stress, and expected total stress computed from the imposed driving body force from the top of the domain. The expected total shear stress at height z is calculated as below,

$$(L_z - \mathrm{MAX}(z,h) + \mathrm{MAX}(0,h-z)(1-\lambda_p)) \left(-\frac{\partial P}{\rho \partial x}\right), \quad \text{for CSA,} \tag{8a}$$

$$(L_z - \mathrm{MAX}(z,h) + \mathrm{MAX}(0,h-z)(1-\lambda_p)) \left(-\frac{\partial P}{\rho \partial x}\right) / (1 - \mathrm{MAX}(0, \mathrm{SIGN}(h-z))\lambda_p), \quad \text{for ISA,} \tag{8b}$$

where L_x, L_y and L_z are the dimensions of the computational domain, z is the vertical coordinate, h is the height of the cubes, λ_p is the packing density, MAX() is the max function which returns the largest value from the numbers provided, SIGN() is the sign function which returns the sign of the number provided. Eq. 8b confirms that the

expected total shear stress for ISA has an abrupt increase at the cube height h (see Fig. 2), whereas Eq. 8a confirms that it has no abrupt change at $z = h$ for CSA.

Fig. 2a shows data from the CSA approach. The vertical profile of the expected total stress below the cuboid height shows a slightly slower change of the slope than above the canopy as a constant body force is applied in the fluid region only and the ratio of the fluid volume to the total volume within the canopy is 67%. The viscous stress is negligible except near the cuboid height and near the floor surface. The dispersive stress immediately below the cuboid height is much greater than that above the canopy. The contribution of the integrated drag stress to the total shear stress is dominant below z/h = 0.5. The time- and spatial-average of the CSA is about 30% less than the ISA data (see Fig. 2b) because the packing density is 33%. The total stress in Fig. 2a matches very well with the expected total stress, except for a small peak at the cuboid height which is owing to the finite number of the discretised slices over the cuboid height. The normalized maximum total stress is slightly less than unity again because the constant pressure gradient $-\delta_{i1}\frac{\partial}{\partial x_i}\left(\frac{P}{\rho}\right)$ was applied in the fluid region only. For a greater domain height to block height ratio, the normalized maximum total shear stress would be closer to unity.

Fig. 2b shows vertical profiles of normalized shear stresses which were obtained in the same way as for those in Fig. 2a except that the ISA is used throughout. The total stress profile shows a significant abrupt change at the cuboid height, where is an evident discontinuous point. This is simply because the average area, which is used to calculate the stress with a unit m^2s^{-2}, changes by 33% at the cuboid height while the total shear force with a unit m^4s^{-2} varies continuously across the entire height of the domain. In other words, the evident discontinuity in the ISA profiles is because of the discontinuity of the geometry of the solid part at the canopy height. On the contrary, using the CSA approach, this issue does not occur. Fig. 2a shows a continuous change of the total shear stress where the average area is constant over the entire domain height L_z. In Fig. 2b the profile of the expected total stress shows a significant abrupt change at the cuboid height as well. Again Eq. 8 confirms this.

It is to be noted that the most crucial implication is that the ISA would yield overestimated shear stresses and momentum sinks (drag) in a one-dimensional column urban model, if such a model does not take account of the solid parts of the canopy. A plot of a vertical profile of the body force implemented in the one-dimensional column models is unlikely able to show this potential issue. For some realistic urban geometry (e.g. Xie and Castro, 2009) with the ratio of solid area to fluid area at a horizontal plane decreases gradually to zero at the canopy top, such 'discontinuous' or 'step change' point of the vertical profiles of stresses does not occur.

Fig. 2b shows that the normalized maximum shear stress at the floor is approximately 1.5. This is far greater than unity which would be expected for the ISA approach. Again, this is because the total shear force over the entire plane at various height changes continuously while the average area changes by 33% at the cuboid height. For canopies with larger packing densities, larger differences of the total shear stress within the canopy between the ISA and CSA estimates would be expected. For example, the DAPPLE site in central London (e.g. Xie and Castro, 2009) has a packing density of about 50%, which is not untypical of city centres. More attention

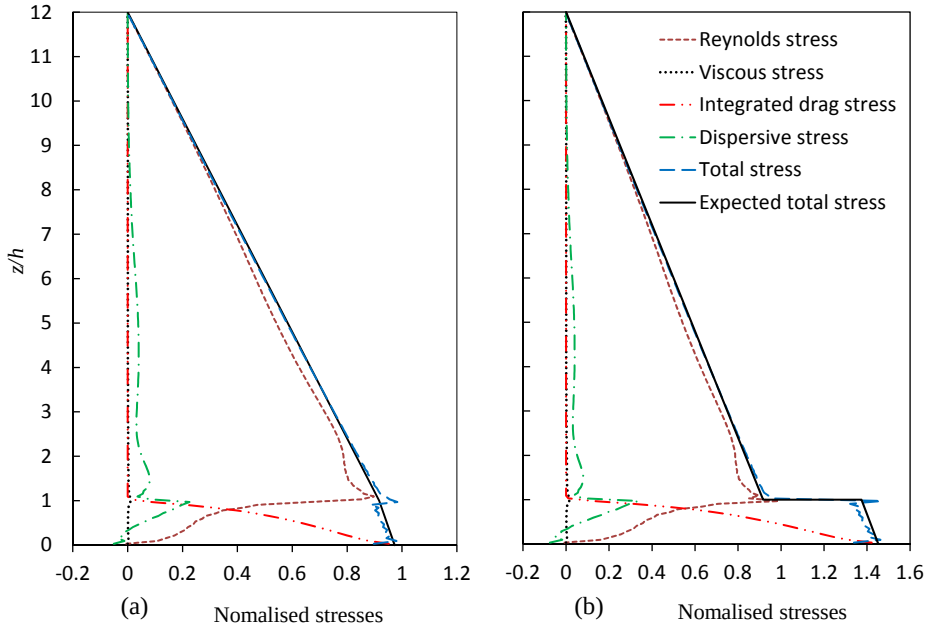

Fig. 2 Vertical profiles of time- and spatially-averaged total shear stress, Reynolds shear stress, dispersive stress, integrated drag stress which was converted from integrated drag calculated from the top of the cuboid height, viscous shear stress, and expected total stress which is computed from the imposed driving body force from the top of the domain. All of the stresses are normalized by $-L_z\delta_{i1}\frac{\partial}{\partial x_i}\left(\frac{P}{\rho}\right)$, where $\delta_{i1}\frac{\partial}{\partial x_i}\left(\frac{P}{\rho}\right)$ is the specified constant pressure gradient in the fluid region. h is the block height. (a) CSA; (b) ISA.

needs to be paid on the dispersive stress, since it is calculated from a spatial average. An inappropriate spatial average may lead to a seriously biased interpretation of the dispersive stress. However, because it is difficult to get a drag distribution over the building height and the momentum flux budget, potential errors due to the ISA approach for a complex urban geometry are more difficult to identify for a simple idealised geometry.

In summary, the potential issue of the ISA for parametrization of a one-dimensional column urban model is the overestimated magnitude of the normalized total shear stress, Reynolds shear stress, dispersive shear stress, drag coefficient, heat source and scalar source within the canopy.

It is interesting that these problems have not recieved much attention previously. The first reason might be that the spatially averaged stresses were first and mainly used to parametrize flows within and above the one-dimensional plant canopy, for which the packing density is much smaller than the urban geometry, and with a ratio of the solid part to the fluid part at a given horizontal plane changing gradually to

zero at the canopy top. The second reason might be that for urban flows over idealised geometries, smaller packing density is usually used, such as 25% (e.g. Coceal et al., 2006; Xie et al., 2008). This leads to smaller differences in the data calculated through the ISA and CSA. The third reason might be that only recently has parametrization of urban flows for one-dimensional column models with a few grid points within the canopy become of particular interest.

4 Conclusions and discussion

Parametrization of urban flows within the canopy is of great interest. In particular, more recently the use of one-dimensional multi-layer models in mesoscale models are being developed. The paper aims to address the risk of using intrinsic spatial averaging (ISA) in processing of building resolved computation data to supply parametrization of the canopy flows in such models.

Using a simple test case with a packing density 33%, we have demonstrated that the ISA yields greater total shear stress within the urban canopy and a more abrupt change of total shear stress at the canopy height, compared to comprehensive spatial averaging (CSA). We would like to emphasize that this is an issue only if the urban column model does not account explicitly for the volume of the buildings, and we trust that none of the current most important multilayer urban column models do such an error.

The CSA results confirm that the total vertical momentum flux of the entire domain (i.e. the total shear force) is continuous within and above the urban canopy, regardless of the packing density, or whether the urban geometry changes abruptly. The CSA approach is useful for extremely complex scenarios, such as in a plant canopy or in porous material, where it might be too difficult to estimate the solid volume, it would be more sensible to calculate the shear stresses based on the total area including both fluid and solid parts. The CSA approach is also useful to calculate the global shear stresses over irregular rough wall while the details of the roughness elements are not able to be resolved. Usually the total area of a plane including solid and the fluids part is used to calculate the shear stresses.

The one-dimensional column models of urban flows will benefit from the CSA approach. An accurate estimation of the body forces (i.e. the drag which takes into account the effects of buildings) imposed at various layers in these models is crucial. It is to be noted that the ‘typical’ way to estimate the body force is to use the mean wind speed within the canopy and a drag coefficient, which are usually difficult to obtain. The CSA approach is able to provide an alternative way. At a certain height, the body forces can be converted from the increment at that height of the vertical profile of integrated drag stress of the CSA data (Fig. 2a) given that the integrated drag stress at the ground surface is known and a vertical profile of the integrated drag stress is approximated. It is to be noted that at the ground surface the integrated drag stress is equal to the total shear stress (Fig. 2a). Therefore, the key is to have an appropriate estimation of the total stress at the ground surface. A further discussion of an approximation of the total surface shear stress and the shape of the vertical profile of the integrated drag stress is beyond the scope of this paper.

It is to be noted that we do not imply that the ISA procedure is inappropriate. Certainly the ISA has a clear physical meaning, e.g. its focus on the local fluid field within the urban canopy. If the averaging of ISA is properly done, and the parameterizations are coherent with the averaging technique chosen, then the global momentum conservation for a one-dimensional column model is satisfied. On the other hand, the CSA implicitly satisfies the global momentum conservation. Although we would not recommend replacing the ISA with the CSA entirely, we would suggest that the CSA is preferred if a parametrization is needed for one-dimensional column urban models.

This paper focuses on time- and spatially-averaged shear stresses (i.e. vertical momentum fluxes) in urban environments for one-dimensional column urban models. We believe for dealing with heat and passive scalar fluxes, using the CSA approach will have the same benefit as dealing with the momentum fluxes. It is most important to consider the time- and spatially-averaged vertical fluxes if one-dimensional urban models are concerned. In some applications volume average quantities obtained from the ISA approach are also of interest. Nevertheless, if an estimation of the local velocities, temperature and scalar concentration etc. within the urban canopy is of greater interest, only building geometry resolved models (such as computational fluid dynamics models) are able to give a reasonable estimation of these quantities. This can be achieved by coupling with the meso-scale models, but at the cost of a very large computation.

Acknowledgements The work is funded by the UKs Engineering and Physical Sciences Research Council grants EP/K04060X/1 (Southampton). ZTX is grateful to Prof Ian Castro, Drs Omduth Coceal and Glyn Thomas for useful discussions. We also appreciate the helpful comments from the two anonymous reviewers. All of the computations were done on the IRIDIS supercomputer, University of Southampton.

References

Castro IP, Xie ZT, Fuka V, Robins AG, Carpentieri M, Hayden P, Hertwig D, Coceal O (2016) Measurements and computations of flow in an urban street system. Boundary-Layer Meteorol 162:207–230

Coceal O, Thomas TG, Castro IP, Belcher SE (2006) Mean flow and turbulence statistics over groups of urban-like cubical obstacles. Boundary-Layer Meteorol 121:491–519

Fernando HJS (2010) Urban atmospheres in complex terrain. Annu Rev Fluid Mech 42:365–89

Finnigan JJ (2000) Turbulence in plant canopies. Annu Rev Fluid Mech 32:519–571

Gray WG (1975) On the theorems for local volume averaging of multiphase systems. Int J Multiphase Flow 3:333–340

Gutierrez E, Gonzalez J, Martilli A, Bornstein R, Arend M (2015) Simulations of a heat-wave event in New York City using a multilayer urban parameterization. J Appl Meteorol Climatol 54:283–301

Husain S, Blair S, Mailhot J, Leroyer S (2013) Improving the representation of the nocturnal near-neutral surface layer in the urban environment with a mesoscale atmospheric model. Boundary-Layer Meteorol 147:525–551

Inagaki M, T TK, Nagano Y (2005) A mixed-time-scale sgs model with fixed model parameters for practical les. J Fluid Eng 127:1–13

Kondo H, Genchi Y, Kikegawa Y, Ohashi Y, Yoshikado H, Komiyama H (2005) Development of a multi-layer urban canopy model for the analysis of energy consumption in a big city: Structure of the urban canopy model and its basic performance. Boundary-Layer Meteorol 116:395–421

Martilli A (2002) Numerical study of urban impact on boundary layer structure: sensitivity to wind speed, urban morphology, and rural soil moisture. J Appl Meteorol 41:1247–1266

Martilli A, Santiago JL (2010) A dynamic urban canopy parameterization for mesoscale models based on computational fluid dynamics reynolds-averaged navierstokes microscale simulations. Boundary-Layer Meteorol 137:417–439

Masson V, Seity Y (2009) Including atmospheric layers in vegetation and urban offline surface schemes. J Appl Meteor Climatol 48:1377–1397

Nikora V, McEwan I, McLean S, Coleman S, Pokrajac D, Walters R (2007) Double-averaging concept for rough-bed open-channel and overland flows: Theoretical background. J Hydraul Eng 133:5873–883

Raupach M, Coppin PA, Legg BJ (1986) Experiments on scalar dispersion within a model plant canopy. part i: The turbulence structure. Boundary-Layer Meteorol 35:21–52

Raupach MR, Shaw RH (1982) Averaging procedures for flow within vegetation canopies. Boundary-Layer Meteorol 22:79–90

Santiago JL, Martilli A (2007) Cfd simulation of airflow over a regular array of cubes. part ii: analysis of spatial average properties. Boundary-Layer Meteorol 122:635–654

Sharma A, Fernando H, Hamlet A, Hellmann J, Barlage M, Chen F (2017) Urban meteorological modeling using WRF: a sensitivity study. Int J Climatol 37:1885–1900

Slattery JC (1999) Advanced transport phenomena. Cambridge University Press, Cambridge CB2 2RU, UK. pp 200

Wilson NR, Shaw RH (2007) A higher order closure model for canopy flow. J Appl Meteorol 133:5873–883

Xie ZT, Castro IP (2009) Large-eddy simulation for flow and dispersion in urban streets. Atmos Environ 43:2174–2185

Xie ZT, Coceal O, Castro IP (2008) Large-eddy simulation of flows over random urban-like obstacles. Boundary-Layer Meteorol 129:1–23

Yuan J, Piomelli U (2014) Roughness effects on the reynolds stress budgets in near-wall turbulence. J Fluid Mech 760:R1–12